Three-Axis Fiber Laser Magnetometer

G.A. Cranch, G.A. Miller, C.G. Askins, R.E. Bartolo, and C.K. Kirkendall
Optical Sciences Division

Introduction: Acoustic detection of targets in shallow water environments is difficult due to high levels of anisotropic acoustic background noise. Detection range can be improved by simultaneously measuring non-acoustic signatures such as electromagnetic fields. A fiber laser vector magnetometer has been developed for seabed-mounted surveillance arrays. Three orthogonally mounted sensors measure each component of the Earth's field. Perturbations within these signals enable detection and tracking of remote targets.

Sensor Operating Principle: The sensor operates by converting a magnetic field into mechanical strain in a fiber laser sensor through the Lorentzian force.[1,2] A single-frequency, distributed-feedback (DFB) fiber laser is attached to a conducting ribbon carrying an AC current, i. In the presence of a magnetic induction, B, the ribbon experiences the Lorentzian force given by $F = B \bullet i$, causing it to oscillate at the AC frequency, thereby inducing strain in the fiber laser. The concept is illustrated in Fig. 1. Here, a gold-coated fiber laser is soldered to an aluminum ribbon, which is fixed in place, under tension, by aluminum clamps. Setting the AC frequency to a mechanical resonance of the ribbon

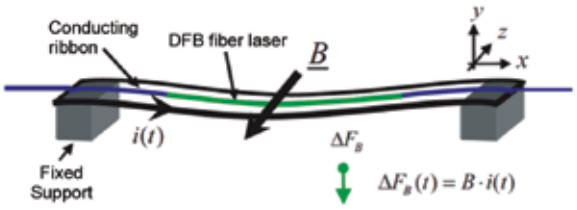

FIGURE 1
Operating principle of the sensor.

provides greater than 40 dB of signal amplification. The response of the sensor, expressed in terms of the component of the laser frequency modulation amplitude at the dither frequency, is given by

$$\Delta\nu \propto i \bullet B \bullet Q, \qquad (1)$$

where Q is the mechanical quality factor of the resonant sensor. The laser frequency shifts are measured interferometrically.[1] The dither frequency is actively adjusted to track the mechanical resonance, which may shift slightly due to changes in ambient temperature. A miniature induction coil in the sensor provides a means of applying a bias field to compensate for the Earth's field, alleviating the dynamic range requirements of the interrogation system when attempting to measure nanotesla (nT) perturbations on a field that may exceed 10^5 nT. The resolution of the sensor, limited by thermomechanical noise in the oscillator, is currently 1 nT/Hz$^{1/2}$ at 1 Hz for an rms-current of 75 mA. Further improvement in the sensitivity can be achieved by increasing the mechanical-Q. A prototype magnetometer is shown in Fig. 2 (top right).

Three-Axis Magnetometer Node: This sensor has been developed into a remotely deployable, 3-axis magnetometer for undersea deployment. A sensing node incorporates three orthogonally mounted magnetometers and an optically powered microelectromechanical systems (MEMS)-based inclinometer. The deployed orientation of the node can be determined from a bearing obtained by the 3-axis magnetometer and inclinometer. The node is pressure tolerant to greater than 100 m depth and comprises an anodized aluminum base and acrylic dome. The instrumentation is mounted onto an additional aluminum plate and secured to the base. The instrumented node is shown in Fig. 2. The MEMS inclinometer is powered by a capacitor bank trickle-charged from a photonic power converter (PPC). The dither current for the magnetometers is supplied by a second PPC configured for high current generation into a low impedance load. A 2-W, 810-nm laser diode provides the MEMS power through a multimode fiber, and two 1480-nm laser diodes provide power for the dither current. As this system is optically powered, no additional electrical power is delivered to the node. A 1-km fiber-optic cable separates the node and electronics, which can be increased to several kilometers. The total separation distance is limited by the transmission loss of the 810-nm signal. A parallel effort has developed an all-optical inclinometer based on multicore fiber,[3] shown in Fig. 2 (far right). This would replace the MEMS inclinometer and enable an increase in the standoff distance to greater than 10 km.

Magnetic Field Measurements: Figure 3 shows the output of two orthogonal magnetometer axes aligned in a plane approximately parallel to the Earth's surface. The absolute measured levels reflect the local field experienced in the laboratory. The observed perturbations on this field correspond to a permanent magnet passing by the node. The characteristics of a moving dipole, resolved onto two orthogonal axes, are clearly visible in the measured data.

Summary: Fiber-optic sensors offer the benefits of remote interrogation and ease of multiplexing. A fiber laser-based sensor system has several advantages over

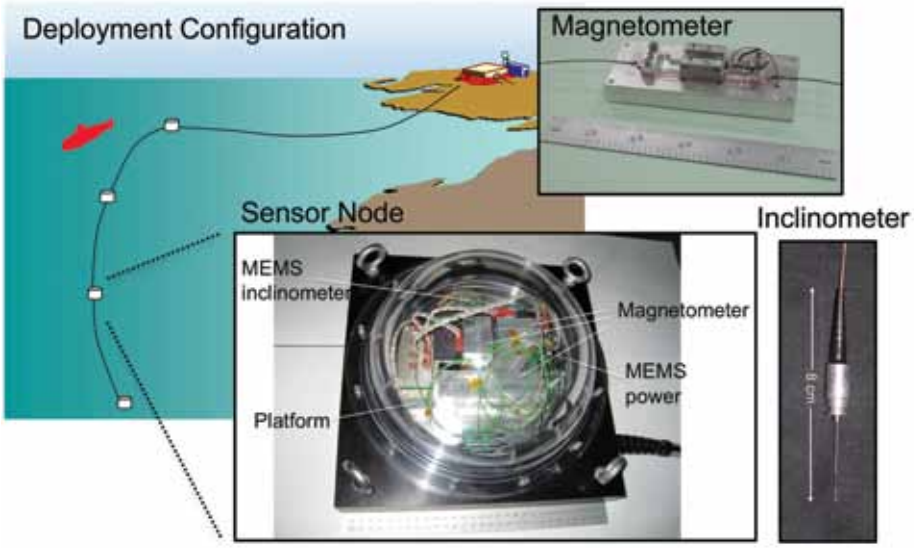

FIGURE 2
Magnetometer array deployment configuration, sensor node, all-optical inclinometer, and magnetometer.

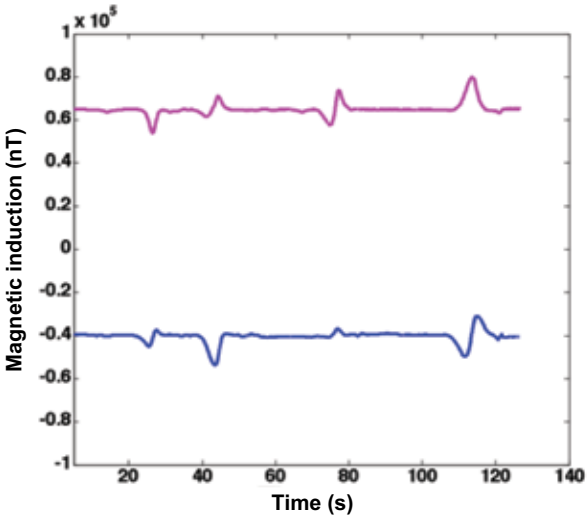

FIGURE 3
Output of two sensors showing magnetic perturbations.

previous fiber-optic magnetic field sensors. The Lorentzian force is a highly linear transduction mechanism, and the sensor exhibits no measurable hysteresis. This permits open loop operation, dramatically simplifying the sensor head. Increasing the dither current yields a proportional increase in responsivity and hence sensitivity. This novel technique further reduces the amount of electronics required in the sensor head, increases the permissible distance between the sensor and optoelectronics unit, and reduces the power requirement. Furthermore, the sensor contains no magnetic material, enabling its use in high field environments. Additionally, the system can be integrated with existing seabed-mounted fiber-optic hydrophone arrays[4] to form multiparameter sensing arrays, increasing effectiveness in noisy acoustic environments.

[Sponsored by ONR and the Navy International Programs Office]

References

[1] G.A. Cranch, G.M.H. Flockhart, and C.K. Kirkendall, "High-resolution Distributed Feedback Fiber Laser DC Magnetometer Based on the Lorentzian Force," *Meas. Sci. Tech.* **20**, 034023 (2009).

[2] G.A. Cranch, G.M.H. Flockhart, and C.K. Kirkendall, "Distributed Feedback Fiber Laser Strain Sensors," *IEEE Sensors Journal* **8**(7), 1161–1172 (2008).

[3] G.A. Miller, C.G. Askins, and G.A. Cranch, "Interferometric Interrogation of a Multicore Fiber, Two-axis Inclinometer," *Proc. SPIE* **7503**, 75032R (2009).

[4] C.K. Kirkendall and G.A. Cranch, "Fiber-optic Bottom-Mounted Array," *2003 NRL Review*, pp. 189–191 (2003).

Navigating Using Spiral Sound

B.R. Dzikowicz[1] and B.T. Hefner[2]
[1]*Acoustics Division*
[2]*Applied Physics Laboratory, University of Washington*

Introduction: With the increased use of underwater robotics in both Navy and commercial applications, underwater navigation becomes more and more important. As researchers attempt to make these vehicles smaller and less expensive, simple systems for the navigation of multiple vehicles become important. A research team from the Naval Research Laboratory

in collaboration with the Applied Physics Laboratory at the University of Washington in Seattle, Washington, and the Naval Surface Warfare Center in Panama City, Florida, are developing and testing an underwater navigation system that uses a spiral-shaped acoustic wave to determine aspect. The single, stationary beacon can provide a navigation signal for any number of underwater vehicles.

Navigating with Spirals: Navigation by the satellite Global Positioning System (GPS) has become ubiquitous in modern life. Receivers are available for cars, boats, and even cell phones. These systems can be accurate to within a few meters. Differential GPS (DGPS), which uses a fixed antenna as a reference, can be accurate to within a centimeter. Unfortunately, GPS signals cannot penetrate the water's surface. Thus, various acoustic and inertial techniques have been developed for underwater navigation. Inertial techniques include accelerometers, like those popular in gaming consoles, and gyroscopic compasses that can determine position by judging how the vehicle is moving relative to the Earth. One acoustic technique available, known as "long-baseline," uses the distances to fixed sound sources, determined from the time it takes the sound to reach the receiver, to triangulate to the receiver's position. Another popular acoustic technique, called "ultra-short baseline" navigation, measures the arrival of a single incoming signal using several hydrophones (underwater microphones) positioned on the same vehicle.

The research team's navigation technique differs from the baseline techniques because the signal coming out of the beacon itself varies with aspect, thus only a single hydrophone is required. Consider the pattern of concentric circles made on the surface of a pond after a pebble is tossed in. These peaks and troughs are known as wave fronts and they travel out from a central source at a fixed speed. Under the water's surface, sound waves can easily be made to form circular wave fronts, analogous to the pebble in the pond. The research team developed another type of wave front, a spiral wave front, where, instead of concentric circles, there is one continuous spiral-shaped front emanating from the source. Figure 4 shows a spiral wave front and its source collocated with a circular wave front. Note in this figure that the distance between the circular and spiral wave fronts does not change along a particular direction. Thus, if a hydrophone is placed at some position around the beacon, the aspect angle relative to the beacon can be determined by comparing the arrival of the different wave fronts. This navigation technique is also used by aircraft navigation and is called VHF Omnidirectional Range (VOR). However, VOR uses radio signals rather than sound waves.

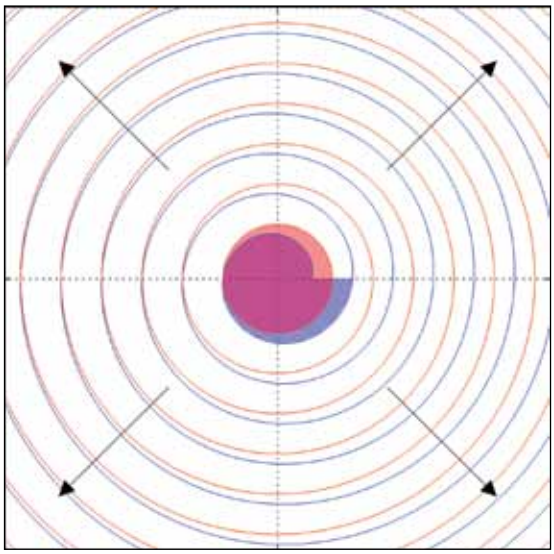

FIGURE 4
Spiral wave front beacon generating circular wave fronts in blue and a spiral wave front in red.

Testing on a Radio-Controlled Boat: Thomas Howarth at the Naval Undersea Warfare Center in Newport, Rhode Island, built a beacon based on this concept. To test the accuracy of the beacon, it is attached to a dock on a pond about 3 m below the water's surface at the Naval Surface Warfare Center in Panama City, Florida. A remote-controlled (RC) pontoon boat is equipped with a hydrophone below the water's surface to determine aspect from the spiral wave front beacon, and a GPS antenna above the surface deter-

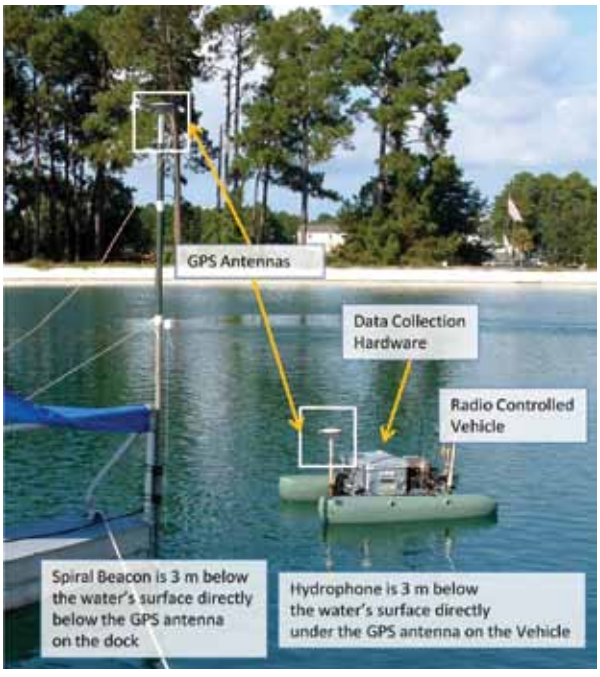

FIGURE 5
Photo of the experimental setup.

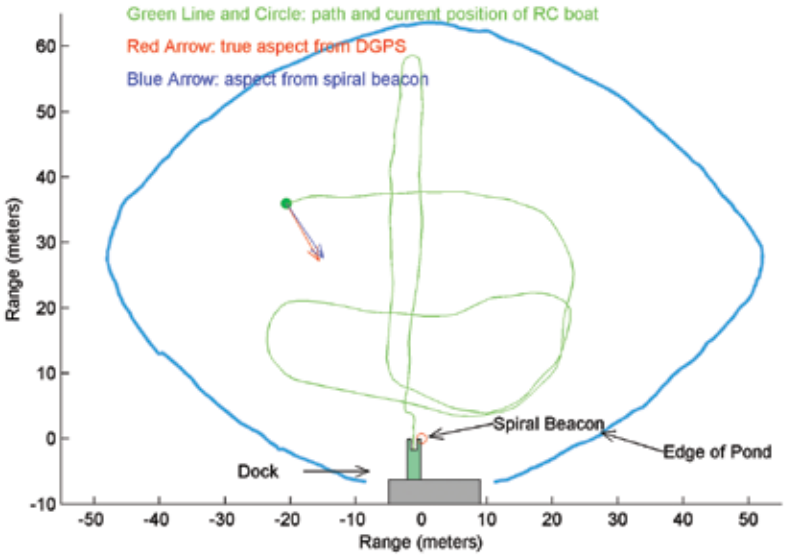

FIGURE 6
Plot showing the position of the RC boat with aspect determination from both the spiral wave front beacon and differential GPS. The green line indicates earlier vehicle positions.

mines aspect using DGPS (see Fig. 5). The RC boat is piloted around a pond and aspect determination from the spiral wave front beacon is compared to the DGPS result. The system takes data from both systems every 2 s. A single measurement is plotted in Fig. 6. The result shows the position of the RC boat and arrows to depict the aspect to the beacon using both the spiral wave front beacon results and the DGPS results. Although not as good as the DGPS results, the beacon is quite accurate, giving an error between 5 and 15 degrees across all of the data. Several different signal processing schemes were tested, some of which worked better in different conditions than others.

The biggest advantage of this system over more traditional baseline techniques is simplicity. A single stationary beacon can be used to navigate any number of remote underwater vehicles. The remote vehicles need only have a single hydrophone available, and can even repurpose one from its sonar or acoustic communications system. With future visions of swarms of underwater vehicles, this can be a huge advantage.

[Sponsored by ONR]

Analysis of the Elasticity of Fibrous Brain Structures Using Sound

A.J. Romano and B.H. Houston
Acoustics Division

Background: The noninvasive evaluation of the elastic properties of the human brain is a very active area of research. This is a promising method of analysis in the sense that if the material properties of the brain can be determined with accuracy, they may provide a valuable metric for the evaluation of its state of health. It has been demonstrated that sound can be used to noninvasively interrogate biological tissues, since the wavelengths of the sound waves in the tissues are directly related to local elastic stiffness values.[1] This method has previously been applied to the brain; however, efforts to date tend to homogenize the brain structures to provide "effective" stiffness and viscoelastic parameters. Here we apply a method that attempts to track waves traveling along white matter pathways such as the cortico-spinal tracts (CST) and the corpus callosum. These structures differ from grey matter in that they are comprised of fiber bundles and can act as waveguides for wave propagation.

Two recent technological breakthroughs enabled the creation of our approach. The first was the development of diffusion tensor imaging (DTI),[2] which provides a mapping of the pathways of fibrous structures based on water perfusion. The second was the development of magnetic resonance elastography (MRE),[1] which provides a measurement of sound waves throughout biological media. Using the fusion of these two measurement methods, we developed an approach called Waveguide Constrained MRE[3] to investigate the elasticity of fibrous structures. Here, we apply this method to the CST of a healthy, 38-year-old male volunteer.

Methods: Waveguide Constrained MRE requires a knowledge of the pathways along which elastic waves may travel and a measurement of the dynamic displacements within the volume surrounding the pathways. Given a knowledge of the position vectors of the pathways, a spatial-spectral filter, in the form of a spatially dependent Radon transform, is applied to the measured displacements in an attempt to identify only

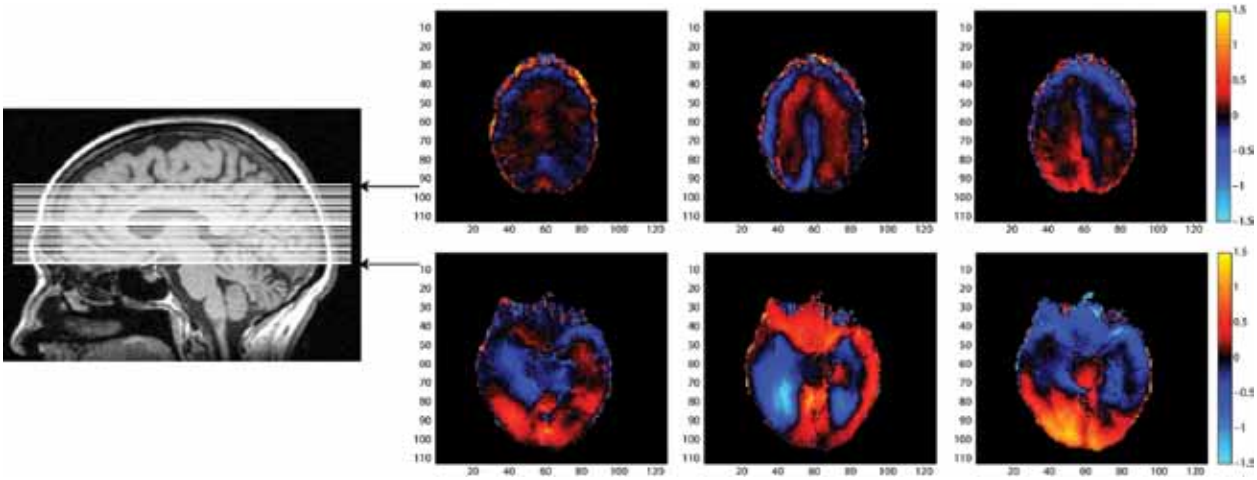

FIGURE 7
MRI of the head and X, Y, and Z displacements at the top and bottom of the field of view.

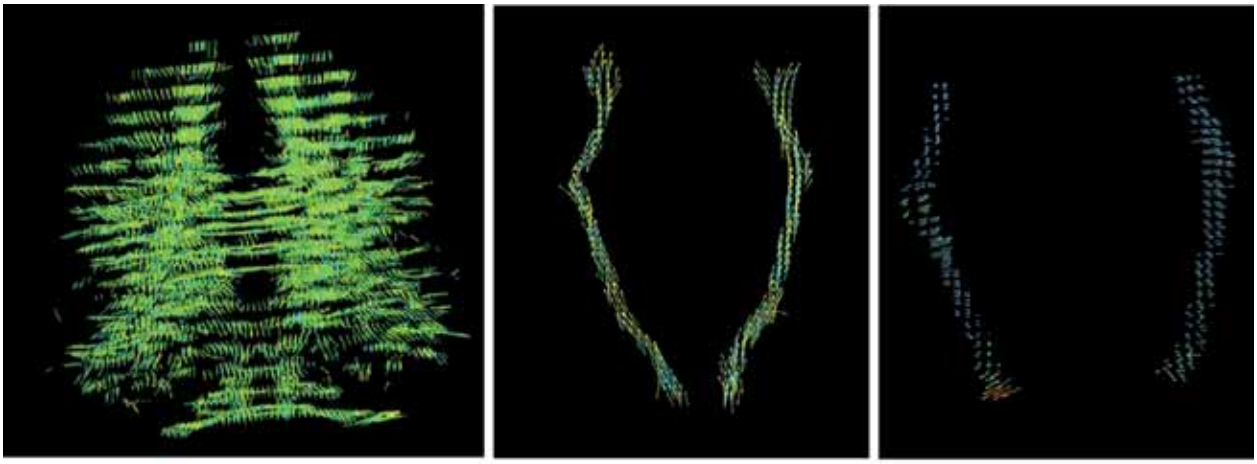

FIGURE 8
(a) DTI of the brain, (b) pathways comprising the CST, and (c) the corresponding filtered shear waves along the CST.

those waves that are traveling parallel along the fiber at every point as if it were a zero-order waveguide mode. Further, a Helmholtz decomposition is performed, which separates the total field into its longitudinal and transverse components. Finally, a sliding window spatial Fourier transform is then applied to these filtered displacements for dispersion analysis, yielding local stiffness values.

For the MRE measurement, the experiment was made using a standard 1.5-T clinical MRI scanner (Siemens, Erlangen, Germany). A head-cradle extended-piston driver was used for 50-Hz harmonic head stimulation. A single-shot spin-echo Echo Planar Imaging (EPI) sequence was used for acquiring three Cartesian components of the wave field in 30 adjacent transversal slices with a 2×2×2 mm^3 isotropic image resolution and eight time steps over the vibration period.

For the fiber position measurement, DTI data were acquired using a single-shot EPI sequence with 12 non-colinear directions. Tensor calculation and tractography along the CST were performed using the tools from the FMRIB Software Library (FSL).

Results: In Fig. 7, we show the MRI of the head as well as the positions of the X, Y, and Z displacement components on the top and bottom of the field of view. In Fig. 8, we show the results from DTI for an evaluation of the fiber pathways comprising the CST, and we show the results of applying the spatial-spectral filter to the MRE data along the CST fibers. In Fig. 9, we show the results of applying a sliding window spatial Fourier transform along two sample fibers for an evaluation of the local shear stiffness values, C_44 and C_55, within the fiber's local reference frame. While estimates for

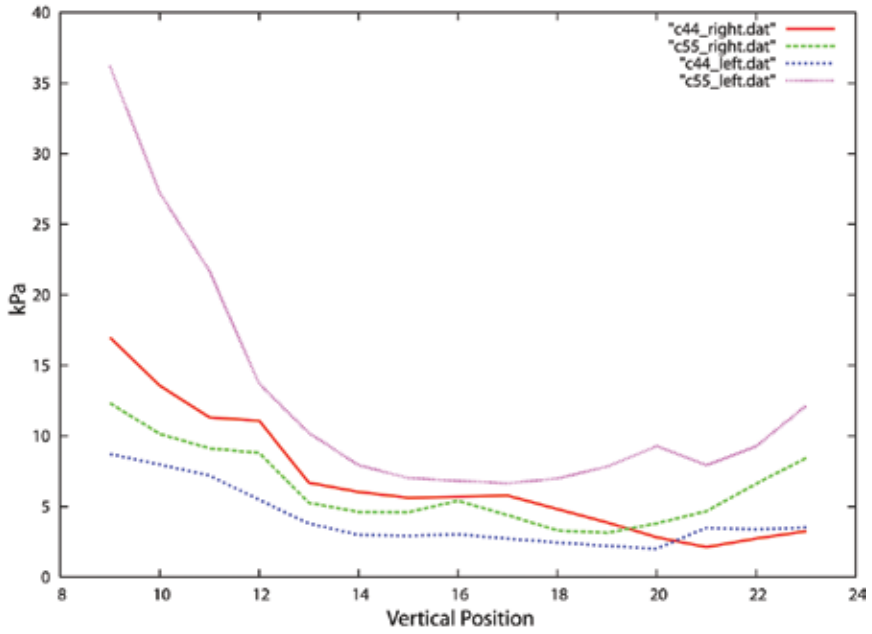

FIGURE 9
Stiffness values for elastic coefficients C_44 and C_55 within the right and left CST.

brain stiffness vary considerably in the literature, average values of around 2 kPa have been reported for the mean shear modulus within slices of healthy samples that include both grey and white matter. Here, the shear stiffness values along the white matter tracts appear to vary from around 2.5 to 10 kPa (i.e., shear wave velocities vary from 1.58 to 3.16 m/s) and are spatially dependent as we follow along the right and left CST from the bottom to the top of the head, while the compressional waves along the fibers have a much higher wave velocity. Future research will apply this approach to other brain structures and at different frequencies.

Acknowledgment: This work was supported by the Office of Naval Research. Thanks to Dr. Ingolf Sack and Dr. Michael Scheel of the Department of Radiology, Charite-Universitatsmedizin, Berlin, Germany for providing all measurements utilized in this work.

[Sponsored by ONR]

References

[1] R. Muthupillai, D.J. Lomas, P.J. Rossman, J.F. Greenleaf, A. Manduca, and R.L. Ehman, "Magnetic Resonance Elastography by Direct Visualization of Propagating Acoustic Strain Waves," *Science* **269**, 1854–1857 (1995).

[2] P.J. Basser, J. Mattiello, and D. Le Bihan, "MR Diffusion Tensor Spectroscopy and Imaging," *Biophys. J.* **66**, 259–267 (1994).

[3] A.J. Romano, P.B. Abraham, P.J. Rossman, J.A. Bucaro, and R.L. Ehman, "Determination and Analysis of Guided Wave Propagation Using Magnetic Resonance Elastography," *Magnetic Resonance in Medicine* **54**, 893–900 (2005).